

## Laboratory Observations of Spontaneous Magnetic Reconnection

J. Egedal, W. Fox, N. Katz, M. Porkolab, K. Reim, and E. Zhang

*Massachusetts Institute of Technology, Plasma Science and Fusion Center, Cambridge, Massachusetts 02139, USA*  
(Received 13 May 2006; revised manuscript received 12 July 2006; published 5 January 2007)

Detailed measurements of spontaneous magnetic reconnection are presented. The experimental data, which were obtained in the new closed Versatile Toroidal Facility magnetic configuration, document the profile evolution of the plasma density, magnetic flux function, reconnection rate, and the current density during a spontaneous reconnection event in the presence of a strong guide magnetic field. The reconnection process is at first slow, which allows magnetic stress to build in the system while the current channel becomes increasingly narrow and intense. The onset of a fast reconnection event occurs as the width of the current channel approaches the ion-sound-Larmor radius  $\rho_s$ . During the reconnection event magnetically stored energy is channeled into energetic ion outflows and a rapid increase in the electron temperature.

DOI: [10.1103/PhysRevLett.98.015003](https://doi.org/10.1103/PhysRevLett.98.015003)

PACS numbers: 52.35.Vd, 52.72.+v

Magnetic reconnection changes magnetic topology in a plasma through breaking and reconnecting magnetic field lines. It is believed that reconnection releases magnetically stored energy that powers solar flares, magnetic storms in the Earth's magnetotail, and internal disruptions in magnetic fusion devices [1–5]. Theoretical investigations have mostly concentrated on understanding the steady state of fast reconnection. It is now widely believed that two-fluid and kinetic effects give rise to the fast time scales of reconnection observed in nature [6].

However, reconnection as observed in nature is explosive, implying that reconnection must be able to transition from slow to fast; the system must be able to accumulate magnetic stress slowly (in the form of a current sheet), then release it quickly. This “trigger problem,” the question of what process causes the spontaneous transition from slow to fast reconnection is still not well understood [7–10].

Until now, experimental observation of spontaneous reconnection has been limited to linear devices [11–13], which all include strong three dimensional (3D) reconnection dynamics. Meanwhile, space observations show that the spatial scale along reconnecting current sheets can be several orders of magnitude ( $10^4$ ) larger than the spatial scale perpendicular to the current sheets [14], implying that reconnection in nature can also occur in systems for which the global structure is mostly two dimensional. Thus, to address the trigger problem in an experiment where the boundary conditions are compatible with both 2D and 3D reconnection (and a variable guide magnetic field), a new magnetic configuration has been implemented in the Versatile Toroidal Facility (VTF) at the PSFC, MIT. Here, we present the first detailed experimental observation of the spontaneous transition from slow to fast reconnection in a toroidally symmetric plasma configuration, documenting the time evolution of the profiles of key plasma parameters.

Figure 1 shows the new closed magnetic geometry in VTF, based on four coaxial coils installed inside the vacuum vessel. The configuration was developed to access fast

reconnection in incompressible plasmas with strong guide magnetic fields. The four coils are suspended (in three locations) by thin stainless steel wires causing minimal disturbance to the plasma. An external coil set produces a guide magnetic field; for the discharge analyzed here a guide magnetic field  $B_g = B_0 R_0/R$  is imposed, with  $B_0 = 44$  mT and  $R_0 = 1$  m.

For plasma production a burst of 20 kW rf power at 2.45 GHz provides the initial breakdown of the Argon gas at  $1 \times 10^{-4}$  Torr. Then, a solenoid at the center of the experiment ( $R = 0.55$  m, not shown in Fig. 1) induces a toroidal electric field of 2 V/m. This field drives currents in the plasma and in the outer conductor of the coaxial loops; the evolution of the coil currents is illustrated in

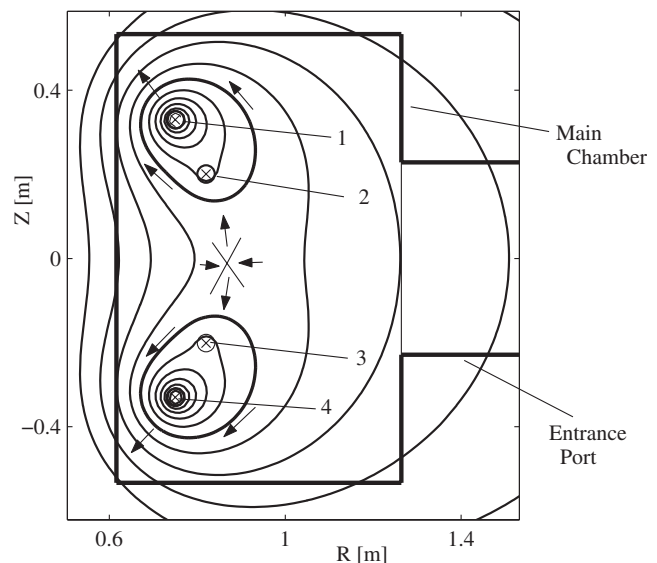


FIG. 1. (a) Cross section of the VTF device including the poloidal projection of vacuum magnetic field lines. The four in-vessel coils are numbered (1 through 4). The arrows indicate the direction of the field line motion during the application of the tearing drive.

Figs. 2(a) and 2(b). After the initial 1 ms period of Ohmic heating the typical plasma density and temperature are on the order of  $n \sim 1.5 \times 10^{18} \text{ m}^{-3}$  and  $T_e \sim 25 \text{ eV}$ , yielding low collisional plasmas where the mean free path for electron-ion collisions is approximately  $\lambda_e \sim 18 \text{ m}$ . However, depending on the ionization fraction, the mean free path for electron-neutral collision is about  $0.5\lambda_e$ .

Magnetic stress is added to the plasma by discharging a capacitor bank (with voltage  $V_{\text{cap}}$ ) connected to the inner conductors of the coax. In Fig. 1 the in-vessel loops are numbered 1 through 4. Let  $\dot{\Psi}_i$  be the value of  $\partial\Psi/\partial t$  evaluated at the surface of the loop  $i$  with radius  $R_i$ ; the wiring of the coaxial loops imposes the relationships  $R_1\dot{\Psi}_1 + R_2\dot{\Psi}_2 + R_3\dot{\Psi}_3 + R_4\dot{\Psi}_4 \sim 0$  and  $R_1\dot{\Psi}_1 - R_2\dot{\Psi}_2 - R_3\dot{\Psi}_3 + R_4\dot{\Psi}_4 \sim V_{\text{cap}}/(2\pi)$ . Thus, as seen in Figs. 2(a) and 2(b), the total current in loops #1 and #4 rapidly increases while the current in loops #2 and #3 decreases when the tearing drive ( $V_{\text{cap}}$ ) is applied.

The induced motion of the flux surfaces points radially into the  $X$  line, and vertically away from the  $X$  line, respectively, as indicated by the arrows in the center of Fig. 1. The reconnection rate remains low initially for  $80 \mu\text{s}$  after the tearing drive is applied. This period is followed by a spontaneous burst of fast reconnection. During the initial  $80 \mu\text{s}$  the plasma current in the center of the cross section increases. As the  $X$  line region becomes more elongated it reaches a critical level of stress after which the plasma current decreases rapidly and the reconnection rate  $E_{\text{rec}} = -(\partial\Psi/\partial t)/R$  jumps from about  $2 \text{ V/m}$  to about  $14 \text{ V/m}$ . This behavior of the plasma current and the loop voltage is illustrated in Figs. 2(c) and 2(d). We notice the large singular spike in the recon-

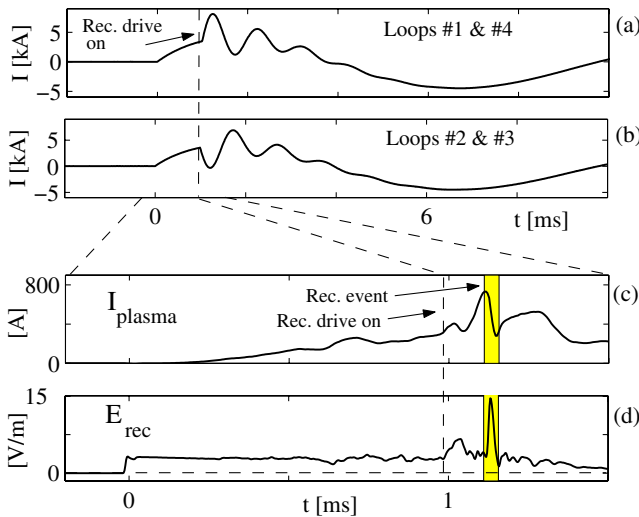


FIG. 2 (color online). (a),(b) Time history of the currents in the four loops, producing the magnetic equilibrium. The rapid modulations of the coil currents at  $t \approx 1 \text{ ms}$  yield the tearing drive illustrated by the arrows in Fig. 1. (c) Total plasma current in the  $X$  line region measured by a Rogowski coil. The rapid fall in the plasma current coincides with the spontaneous reconnection event. (d) Measured  $E_{\text{rec}} = -\partial\Phi/\partial t$  along the  $X$  line.

nection rate similar to sawtooth reconnection in tokamaks and spontaneous reconnection events in nature.

The plasma dynamics are reconstructed from data acquired in a single discharge by electrostatic and magnetic probes. A 196 channel electrostatic probe array provides information on the electrostatic fields and the plasma density for the entire poloidal cross section; the floating potential of the plasma is measured at 98 locations simultaneous with 98 ion-saturation currents measurements. In addition, a novel flux-probe array is used to measure  $\partial\Psi/\partial t$  directly: 98 pickup loops extend across the poloidal cross section. Their widths are proportional to  $R$ , and they are arranged to measure  $\Delta\dot{\Psi}(R, Z) = \dot{\Psi}(R, Z) - \dot{\Psi}(R_0, Z_0) = \int_{R_0, Z_0}^{R, Z} R' \mathbf{B} \times d\mathbf{l}$  on a grid covering the central reconnection region. At the location  $(R_0, Z_0)$  (at the inner vessel wall)  $\dot{\Psi}(R_0, Z_0)$  is measured by a toroidal loop, completing the measurement of  $\dot{\Psi}(R, Z)$ . At a separate toroidal angle  $\Delta\dot{\Psi}(R, Z = 0)$  is measured. The measurements of the reconnection rate at the two toroidal location ( $180^\circ$  apart) prove that the reconnection is mostly axisymmetric. Using Maxwell's equations, the poloidal magnetic fields and the toroidal plasma current density are computed from  $\Psi (= \int \dot{\Psi} dt)$ .

Figure 3 shows the measured contours of the plasma density, electrostatic floating potential, current density, and reconnection rate during a  $65 \mu\text{s}$  time interval. Note that the time intervals between the columns are nonuniform. The dashed magnetic field lines are obtained as the contours of constant  $\Psi$  (directly measured). In the sequence for  $t \leq 75 \mu\text{s}$  the reconnection rate is on the order of  $2 \text{ V/m}$ . In this period the broad current profile is intensified and acquires a significant elongation; the width of the current sheet is reduced to about  $0.1 \text{ m}$ , while the magnetic geometry becomes increasingly stretched.

The profiles at  $t = 80 \mu\text{s}$  mark the onset of the reconnection event. The value of  $E_{\text{rec}} = -(\partial\Psi/\partial t)/R$  jumps to  $14 \text{ V/m}$  at the upper outflow region of the current sheet. Hereafter the elevated value of  $-(\partial\Psi/\partial t)/R$  engulfs the entire reconnection region as the current channel decays away. The highlighted field lines can be followed in time as they move into the  $X$  line, reconnect, and drift apart. The plasma density contours show how the central density is ejected downwards at a velocity consistent with the motion of the highlighted magnetic field lines. The outflow velocity is about  $v_{\text{out}} \sim 11 \text{ km/s}$ , corresponding to an energization of  $\mathcal{E}_{\text{flow}} \sim 24 \text{ eV}$ .

The issue of electron heating has been addressed in separate experiments, applying a miniature ( $\sim 1.5 \text{ cm}^2$ ) Langmuir probe array. The  $IV$  characteristics in Fig. 4(a) were obtained in a single shot by applying discrete biases to its 16 probe tips. The measurements are consistent with Maxwellian distributed electrons in the center of the reconnection region; typically  $T_e$  increases by about  $7 \text{ eV}$  within  $6 \mu\text{s}$  of the onset of reconnection.

The contours of the floating potential (related to the plasma potential through  $\Phi \sim V_f + 4T_e$ ) also undergo

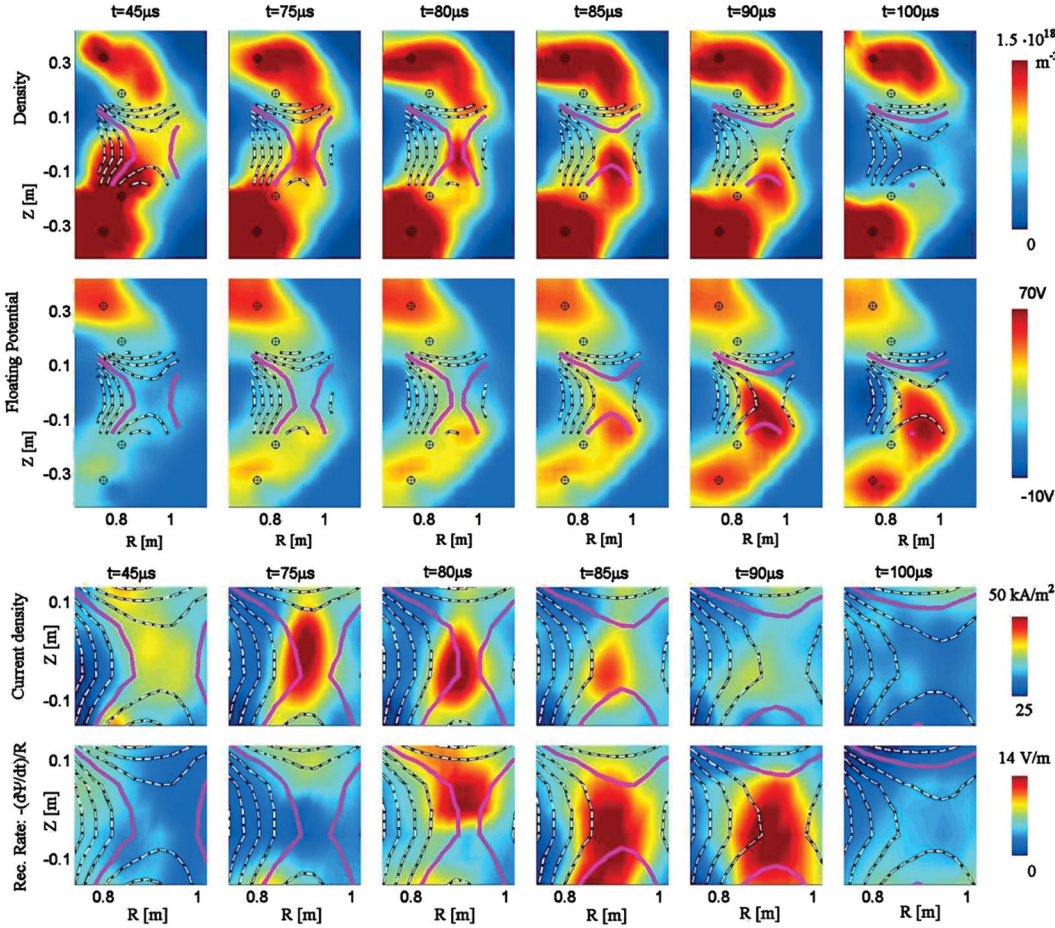


FIG. 3 (color). Measured contours of the plasma density, floating potential, current density, and the reconnection rate. The overlaid lines represent contours of  $\Psi$ , which coincide with the poloidal projection of magnetic field lines. One value of  $\Psi$  is highlighted such that the motion of the field lines can be followed in time. The measurements were obtained in a  $65 \mu\text{s}$  time interval centered about a spontaneous reconnection event. Note that the time steps between the columns are nonuniform.

significant changes during the reconnection event. The potential structure is similar to that measured in the previous VTF open configuration [15]. It develops to maintain  $\mathbf{E} \cdot \mathbf{B} = E_\phi B_\phi + \mathbf{E}_p \cdot \mathbf{B}_p \sim 0$  outside the electron diffusion region (the subscripts  $\phi$  and  $p$  denote the toroidal and poloidal directions, respectively). Because of the free streaming of electrons along the magnetic field,  $T_e$  will be nearly constant along the contours of constant  $\Psi$  in Fig. 3. So when estimating  $\nabla\Phi = \nabla V_f + 4\nabla T_e$ , along a  $\Psi$  contour in the lower outflow region, the  $\nabla T_e$  term may be ignored compared to the large  $\nabla V_f$  term ( $\sim 80$  V over 0.2 m). Thus, the radial electric field across the lower outflow region is about  $|d\Phi/dR| \sim 400$  V/m. Together with the guide magnetic field  $B_\phi \sim 44$  mT this provides an  $E \times B$ -drift  $\sim 9$  km/s, consistent with  $v_{\text{out}}$  obtained above.

The pre-reconnection plasma density and current density across the current sheet are shown in Fig. 4(b), while Fig. 4(c) illustrates the vertical magnetic field  $B_z$  as measured at the midplane ( $Z = 0$  m) as a function of  $R$  before ( $t = 75 \mu\text{s}$  in Fig. 3) and after ( $t = 100 \mu\text{s}$  in Fig. 3) the reconnection event. The reduction in  $B_z$  is caused by the changes in the plasma current profile. Before the onset  $B_{z,\text{up}} = 4$  mT is representative for the upstream magnetic field (the in-plane magnetic field evaluated just outside the current channel in the inflow region). Applying this value we find that the relevant Alfvén speed is about  $v_A =$

$B_{z,\text{up}}/\sqrt{nm_i\mu_0} \sim 10$  km/s (note that the energy in the guide magnetic field cannot be tapped by reconnection, and does not contribute to the relevant Alfvén speed). The inflow speed of the poloidal magnetic field is  $v_{B,\text{in}} = E_{\text{rec}}/B_{z,\text{up}} \sim (14 \text{ V/m})/(4 \text{ mT}) = 3.5$  km/s emphasizing the high rate of reconnection with  $v_{B,\text{in}}/v_A \sim 0.35$  and  $v_{\text{out}}/v_A \sim 1.1$ .

Figure 5 shows  $E_{\text{rec}}$ ,  $n$ , and  $j$  evaluated at the  $X$  line as a function of time;  $t = 0$  coincides with the application of the tearing drive. We notice the very abrupt onset of the fast reconnection event at  $t \sim 80 \mu\text{s}$ ; the spontaneous increase

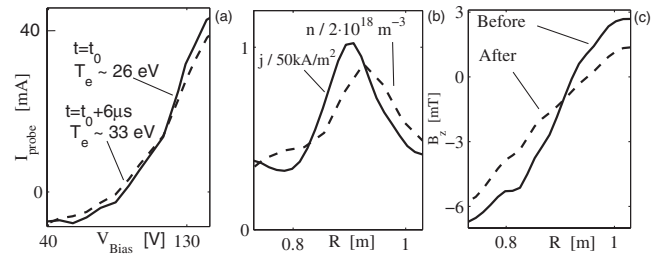


FIG. 4. (a) Typical change in the Langmuir  $IV$  characteristic over a  $6 \mu\text{s}$  interval just after the onset of fast reconnection. (b) Plasma current and density evaluated at the midplane just before the reconnection event. (c) Vertical magnetic field evaluated at the midplane before and after the reconnection event.

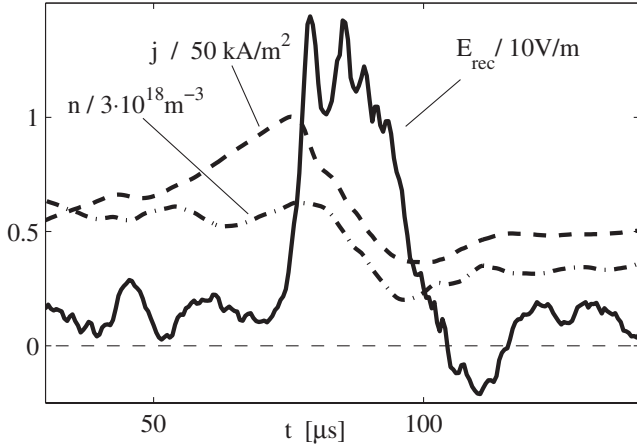


FIG. 5. Time evolution of  $E_{\text{rec}}$ ,  $n$ , and  $j$  at the  $X$  line.  $t = 0$  represents the application of the tearing drive.

in  $E_{\text{rec}}$  appears in a time interval of only  $3 \mu\text{s}$ . Again, it is seen how the jump in the reconnection rate is induced by the change in  $dj/dt$ . The subsequent density decline is consistent with the plasma flowing together with the reconnected flux out of the reconnection region.

During the event the reconnection rate jumps from  $E_{\text{rec}} \approx 2 \text{ V/m}$  to about  $E_{\text{rec}} \approx 14 \text{ V/m}$  while the current is decreasing. The measured current density is in the range of  $50 \text{ kA/m}^2$ , while electron momentum balance by Spitzer resistivity requires  $j \sim 7 \text{ MA/m}^2$ . Evidently, two-fluid effects and/or anomalous resistivity need to be invoked to explain the high rates of reconnection observed.

For the present configuration two-fluid models predict that the ion-sound-Larmor radius,  $\rho_s = \sqrt{m_i T_e / (qB)}$  plays an important role in setting the scale of kinetic Alfvén waves. Interestingly, consistent with recent numerical simulations including a strong guide magnetic field [16], the spontaneous onset of reconnection occurs when the current sheet thickness approaches  $\rho_s \sim 0.08 \text{ m}$ . Furthermore, the ejection of the plasma from the central region is also consistent with a two-fluid picture, where the electron response drives the evolution observed in  $\Phi$ . In turn,  $\partial\Phi/\partial t$  causes radial ion-polarization currents  $j_p$ , that together with the guide magnetic field provides the  $\mathbf{j} \times \mathbf{B}$  force to accelerate the plasma downward, to flow with the  $\mathbf{E} \times \mathbf{B}$  velocity out of the reconnection region.

During the reconnection event the total current through the reconnection region decreases by about  $I = 500 \text{ A}$ . Therefore, the magnetic energy released is about  $0.5LI^2 = 0.5 \times 6 \mu\text{H} \times (500 \text{ A})^2 \approx 0.8 \text{ J}$ , where  $L$  is the self-inductance of the toroidal current channel. We find that the total kinetic energy of the outflow  $\mathcal{E}_{\text{flow}} \times n \times V \sim 24 \text{ eV} \times 2 \times 10^{18} \text{ m}^{-3} \times 0.06 \text{ m}^3 \approx 0.48 \text{ J}$  represents a significant fraction of the magnetic energy available. This rough energy balance indicates that about 60% of the magnetic energy is transferred to kinetic energy in the Alfvénic plasma outflow.

An estimate for the electron heating is given by  $E_{\text{rec}} j \sim 700 \text{ kW/m}^3$ . Meanwhile, the observed increase in the electron temperature only requires a dissipation rate of  $(\Delta T_e / \Delta t) n = (7 \text{ eV} / 6 \mu\text{s}) 2 \times 10^{18} \text{ m}^{-3} = 370 \text{ kW/m}^3$ . This discrepancy (and the early saturation of the electron temperature) is most likely explained by heat losses carried by electrons traveling at  $v_{\text{th}} \sim 3 \times 10^6 \text{ ms}^{-1}$  along field lines out of the reconnection region. Also, the electrons must provide the energy required to drive  $\partial\Phi/\partial t$ , which is responsible for the energetic ion outflow.

In summary, the evolution of the poloidal profiles of the reconnection rate, the magnetic flux function, the plasma density, the current density, and the in-plane electrostatic potential have been documented for the first time during spontaneous reconnection in a highly axisymmetric system. The period of slow reconnection after the tearing drive is applied allows the magnetic stress to accumulate in the system. During this phase a current channel is formed which becomes increasingly intense and elongated. A sudden onset of reconnection is observed as the width of the current sheet approaches the ion-sound-Larmor radius  $\rho_s$ . During the event the plasma in the reconnection region is ejected. Significant electron heating is observed and the evolution of  $\Phi$  indicates that the ions are accelerated to the  $\mathbf{E} \times \mathbf{B}$  velocity (out of the region) by  $\mathbf{j} \times \mathbf{B}$  forces.

The spontaneous reconnection events occur only for a limited range of the plasma parameters available in VTF. Our future studies will map the parameter regimes yielding the spontaneous events. Also, we will study possible 3D effects at the onset of the reconnection events.

This work is partly funded by DOE/NSF Grant No. DE-FG02-03ER54712. W. Fox and N. Katz were funded by the DOE.

- [1] J. W. Dungey, *Philos. Mag.* **44**, 725 (1953).
- [2] J. B. Taylor, *Rev. Mod. Phys.* **58**, 741 (1986).
- [3] V. M. Vasyliunas, *Rev. Geophys. Space Phys.* **13**, 303 (1975).
- [4] S. Masuda *et al.*, *Nature (London)* **371**, 495 (1994).
- [5] R. J. Hastie, *Astrophys. Space Sci.* **256**, 177 (1998).
- [6] J. Birn *et al.*, *J. Geophys. Res.* **106**, 3715 (2001).
- [7] X. Wang and A. Bhattacharjee, *Phys. Rev. Lett.* **70**, 1627 (1993).
- [8] A. Bhattacharjee, K. Germaschewski, and C. S. Ng, *Phys. Plasmas* **12**, 042305 (2005).
- [9] P. L. Pritchett, *Phys. Plasmas* **12**, 062301 (2005).
- [10] P. A. Cassak *et al.*, *Phys. Rev. Lett.* **95**, 235002 (2005).
- [11] P. J. Baum *et al.*, *Phys. Fluids* **16**, 1501 (1973).
- [12] R. L. Stenzel *et al.*, *J. Geophys. Res.* **88**, 4793 (1983).
- [13] A. G. Frank, *Plasma Phys. Controlled Fusion* **41**, A687 (1999).
- [14] T. D. Phan *et al.*, *Nature (London)* **439**, 175 (2006).
- [15] J. Egedal *et al.*, *Phys. Rev. Lett.* **90**, 135003 (2003).
- [16] P. A. Cassak (private communication).